31 Theologis, A., Huynh, T. V., and Davis, R. W., Rapid induction of specific messenger RNA species by auxin in pea pisum-sativum cultivar alaska epicotyl tissue. J. molec. Biol. *183* (1985) 53–68.
32 Vaisius, A. C., and Wieland, Th., Formation of a single phosphodiester bond by RNA polymerase B from calf thymus is not inhibited by α-amanitin. Biochemistry *21* (1982) 3097–3101.
33 White, J. L., and Brakke, M. K., Protein changes in wheat infected with wheat streak mosaic virus and in barley infected with barley stripe mosaic virus. Physiol. Plant Path. *22* (1983) 87–100.
34 Wieland, H., and Hallermayer, R., Über die Giftstoffe des Knollenblätterpilzes. VI. Amanitin, das Hauptgift des Knollenblätterpilzes. Liebigs Ann. Chem. *548* (1941) 1–18.
35 Wieland, Th., Zeitungspapier-Test für Giftpilze. Umschau *78* (1978) 611.
36 Wieland, Th., Peptides of Poisonous Amanita Mushrooms. Ed. A. Rich. Springer, Berlin-Heidelberg-New York 1986.
37 Wieland, Th., 50 Jahre Phalloidin. Naturwissenschaften *74* (1987) 367–373.
38 Wieland, Th., and Fischer, E., Über Elektrophorese auf Filtrierpapier. Naturwissenschaften *35* (1948) 29.
39 Wieland, Th., and Fahrmeier, A., Oxydation und Reduktion an der γ, δ-Dihydroxyisoleucin-Seitenkette des O-Methyl-α-amanitins. Methyl-aldoamanitin, ein ungiftiges Abbauprodukt. Liebigs Ann. Chem. *736* (1970) 95–99.
40 Wieland, Th., and Faulstich, H., Amatoxins, Phallotoxins, Phallolysin and Antamanide: the biologically active components of poisonous Amanita mushrooms. Cr. Rev. Biochem. *5* (1978) 185–260.
41 Wieland, Th., Götzendörfer, Ch., Dabrowski, J., Lipscomb, W. N., and Shoham, S., Unexpected similarity of the structures of the weakly toxic amanitin (S)-sulfoxide and the highly toxic (R)-sulfoxide and sulfone as revealed by proton nuclear magnetic resonance and X-ray analysis. Biochemistry *22* (1983) 1264–1271.
42 Yoshikawa, N., and Takahashi, T., Studies on pathogenesis in viroid infections. 15. Inhibition of hop stunt viroid replication by α-amanitin. Z. Pflanzenk. Pflanzenschutz *93* (1986) 62–71.
43 Zanotti, G., Birr, Ch., and Wieland, Th., Analogs of amanin: synthesis of Ile^{3}-amaninamide and its diastereoisomeric (S)-sulfoxide. Int. J. Pept. Prot. Res. *18* (1981) 162–168.
44 Zanotti, G., Wieland, Th., Benedetti, E., di Blasio, B., Pavone, V., and Pedone, C., Structure toxicity relationships in the amatoxin series. Synthesis of S-deoxy (R)-hydroxy-Ile^{3}-amaninamide, its crystal and molecular structure and inhibitory efficiency. Int. J. Pept. Prot. Res. *34* (1989) 222–228.
45 Zanotti, G., Wieland, Th., d'Auria, G., Paolillo, L., and Trivellone, E., S-deoxo-Abu^{1}, Ile^{3}-amaninamide, an inactive amatoxin analogue. Int. J. Pept. Prot. Res. *35* (1990) 263–270.
46 Zanotti, G., and Wieland, Th., unpublished.

0014-4754/91/11-12/1186-08$1.50 + 0.20/0

Research Articles

Periodicity in fish otolith Sr, Na, and K corresponds with visual banding

H. Seyama, J. S. Edmonds[a], M. J. Moran[a], Y. Shibata, M. Soma and M. Morita

National Institute for Environmental Studies, 16-2 Onogawa, Tsukuba, Ibaraki 305 (Japan), and [a]Western Australian Marine Research Laboratories, P. O. Box 20, North Beach, W. A. 6020 (Australia)

Received 23 November 1990; accepted 13 March 1991

Abstract. Examination of a section of an otolith from a teleost fish by fast atom bombardment-secondary ion mass spectrometry (FAB-SIMS) revealed seasonal periodicity in Sr, Na, and K concentrations that corresponded with visually observed annual banding. Strontium maxima also corresponded with Na and K minima and vice versa. In addition there was a general, apparently age-related, trend in Sr levels, with concentrations at the edge of the otolith being higher than in the core.

Key words. Fast atom bombardment (FAB); secondary ion mass spectrometry (SIMS); fish otolith; calcareous tissues, elemental analysis.

Otoliths are hard, stone-like, non-bony structures which form part of the organs, located in the inner ear, which sense position and motion in vertebrates[1]. In teleost fish, otoliths are made of calcium carbonate in the aragonite crystal form, deposited in a protein matrix[1,2]. Three pairs are present in the labyrinths of each fish of which the sagittae, or sagittal otoliths, are the largest[2]. Two types of information can be obtained from the sagittal otoliths of teleost fish. Firstly, banding evident to the eye or by low-powered microscopy can often provide a method of determining the age of individual fish. The nucleus of an otolith is present at the beginning of larval life, and grows daily by the addition of layers to the outer surface. In sections through an otolith there is usually visible evidence of periodicity in the formation of concentric layers on daily, annual and sometimes intermediate time scales[3,4]. Age-determination of fish is an important part of the study of population dynamics and calculation of sustainable fishery yields. Various hard parts of the fish which show periodic banding, including scales, bones and fin-rays, have been used for this purpose[4]. Otoliths possess the advantage that they continue to thicken by the addition of layers to the medial surface even when the fish has ceased growing. In some fish species the process of age-determination is straightforward, in others the banding is not clear and reading is somewhat subjective. A seasonal variation in chemical composition may provide an improved, more objective means of age determination for such difficult species. Also, if chemical banding, correlated with seasonal environmental changes, was found to be the norm, it could provide a means of validating the conclusions drawn from counting the visible bands.

Secondly, studies of the elemental composition of otoliths, like those of other calcareous tissues of biological origin, such as corals[5], may provide information about past environmental, climatological and oceanographic conditions[6]. In particular, the concentration of Sr in aragonitic carbonate has been shown to be negatively correlated with temperature in both non-biological[7] and biological systems[5], though recently it was claimed that temperature was of no importance in determining the Sr concentration in fish otoliths[8]. If the chemical composition of otolith bands could be shown to reflect environmental variables such as temperature, long-lived fish might be useful as indicators of conditions in the recent past, and fossil otoliths[9] present in sedimentary rocks might well yield information on paleoclimatological and paleooceanographic environments.

Material and methods

In this study we examined the Sr, Na and K concentrations in a fish otolith section by fast atom bombardment-secondary ion mass spectrometry (FAB-SIMS). A section, 1 mm thick, cut to include the nucleus (core), was obtained from an otolith taken from a red emperor (*Lutjanus sebae*) from Western Australian coastal waters (lat. 27°S, long. 113°30′E). The age of the fish was estimated as 27 years by a count of the visual bands within the otolith (fig. 1). After polishing, the sample was cleaned by ultrasonication in water. A CAMECA IMS4f ion microscope with a FAB source was used to record the images and line-scans of positive secondary ions derived from the sample. A detailed description of the FAB-SIMS instrument has been reported[10]. A 15 keV O_2 neutral beam was used to bombard the sample surface, and the secondary ion image was recorded on a resistive anode encoder image acquisition system. When the sample was mounted for analysis, a copper grid of 700 x 500 μm mesh was placed between the sample and the inside face of the sample holder to reduce sample charging.

Results and discussion

Line-scans of $^{23}Na^+$, $^{39}K^+$, $^{40}Ca^+$ and $^{88}Sr^+$ secondary ions were measured by 5-μm step scanning of the sample from the edge to the nucleus across the opaque (light) and hyaline (dark) zones (fig. 1). The area analyzed at each step was 8 μm in diameter. To minimize the effect of sample charging, the intensity ratios of $^{23}Na^+$, $^{39}K^+$ and $^{88}Sr^+$ relative to $^{40}Ca^+$ (matrix element) were calculated and plotted against distance (fig. 2). The charging effect

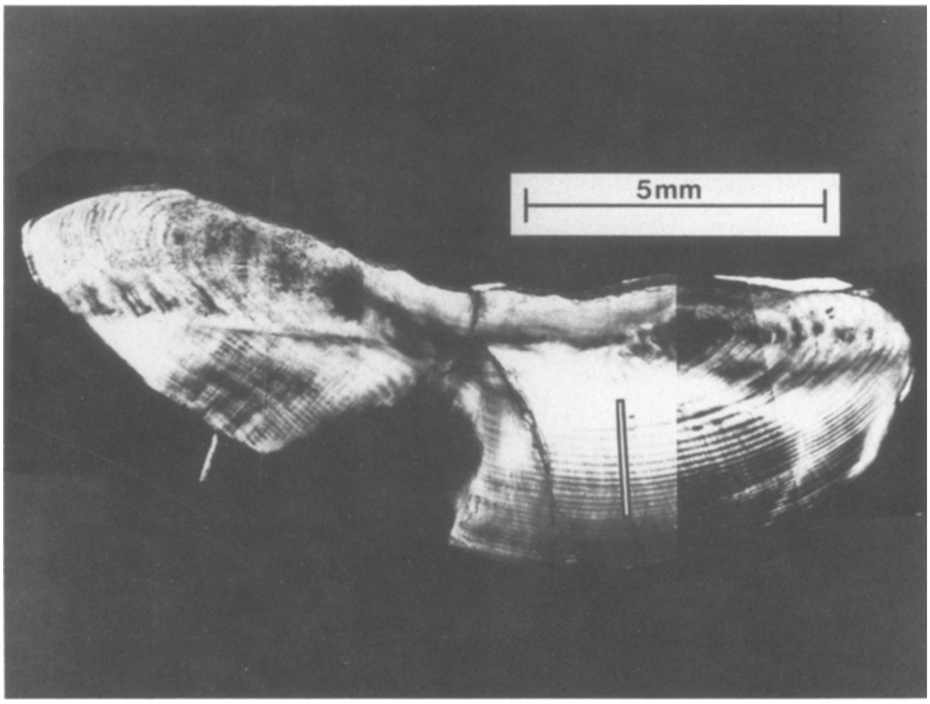

Figure 1. Otolith cross-section showing position of line-scan analysis. Analysis by ICP-AES of whole otoliths from *L. sebae* (n = 5) gave the following elemental concentrations (mean and range): Ca, 38.6%, 37.3–40.3; Na, 4582 mg kg^{-1}, 4344–4884; K, 731 mg kg^{-1}, 704–840; Sr, 1805 mg kg^{-1}, 1772–1916.

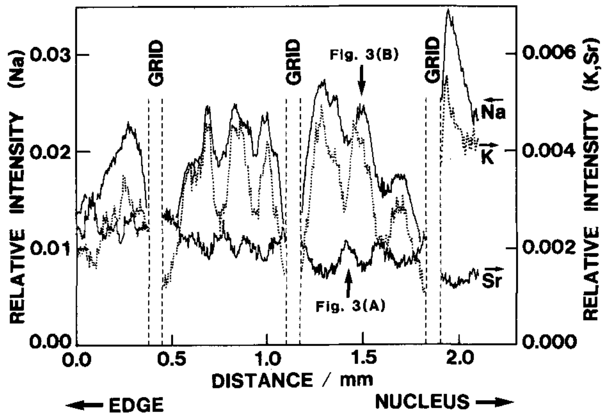

Figure 2. Scans of $^{23}Na^+$, $^{39}K^+$ and $^{88}Sr^+$ along the line indicated in fig. 1. Intensity ratios of three ions to $^{40}Ca^+$ are plotted against distance from edge to nucleus.

for the relative $^{88}Sr^+$ intensity was successfully compensated. However, compensation of the charging effect was insufficient for the relative $^{23}Na^+$ and $^{39}K^+$ intensities. Consequently a reduction in the relative intensities of these two ions was found in the vicinity of the copper grid. It can therefore be assumed that Ca and Sr are contained in the same phase, i.e. the aragonite lattice, and Na and K are contained in another phase, possibly another mineral phase. The total concentration of Na (about 0.45%) and protein (< 1%) suggested that most Na was unlikely to be associated with protein.

Figure 2 shows the variation in the relative concentrations of Na, K and Sr in the sample. Oscillating patterns of relative intensities with a 100–200 µm repeat period, corresponding with the visual bands, were clearly observed. The patterns for Na and K were similar to each other. The repeat period near the edge of the otolith was shorter than that near the nucleus, and again this pattern was consistent with the pattern of opaque and hyaline zones observed in the sample as seen in transmitted light (fig. 1). The concentrations of the three elements showed fluctuations of ± 10–30%. In addition it can be seen that the maximum Sr concentrations corresponded to the minimum Na and K concentrations and vice versa, and that the Sr concentration decreased from edge to nucleus by about 45%. Images of $^{23}Na^+$ and $^{88}Sr^+$ distribution are shown in figure 3; the heterogeneous distribution of these elements, i.e. the microstructure of the otolith, is clearly demonstrated. By using the copper grid as a reference marker it was possible to assign the high Sr, low Na, K zones to the hyaline bands (assumed to result from slower, winter growth[4]; fig. 1), and the low Sr, high Na, K zones to the opaque (summer) bands. Thus the deposition of Sr may well be temperature-related.

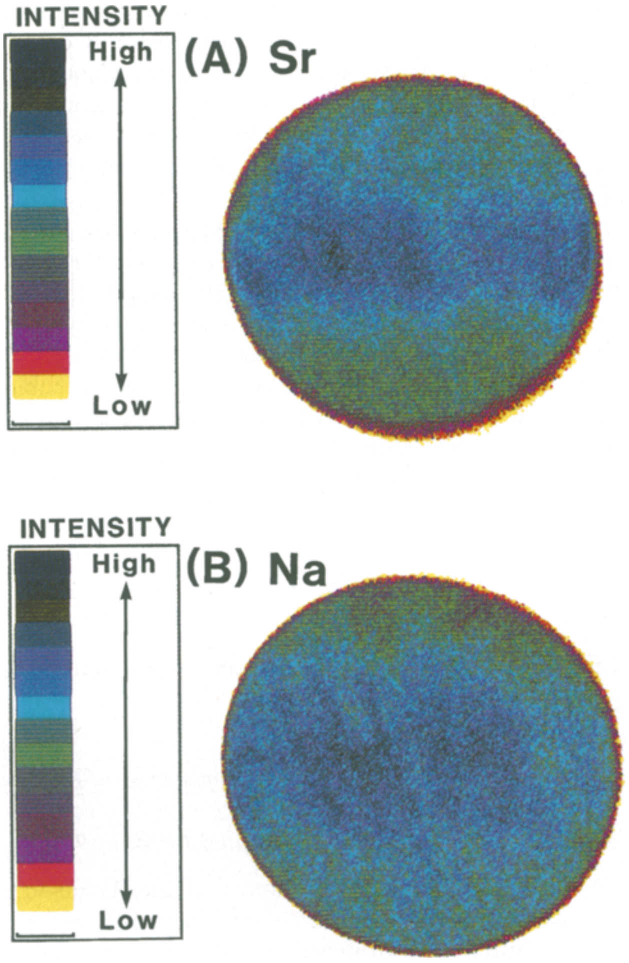

Figure 3. (*A*) $^{88}Sr^+$ and (*B*) $^{23}Na^+$ secondary ion images (250 µm diameter) of area indicated in fig. 2.

Mean concentrations for Sr and Ca in whole otoliths of 1805 $mg\,kg^{-1}$ and 38.6% respectively (from ICP-AES measurements), mean fluctuations in Sr concentration of about ± 12.5% across the otolith (fig. 2) and an annual temperature range of 7 °C (winter, 18 °C; summer, 25 °C) gave, assuming linearity, an approximate relationship of $Sr/Ca\ 10^3 = 8.3 - 0.17\,T$ (°C). This shows a much greater variation of Sr/Ca with temperature in otoliths than for aragonite in non-biological systems ($Sr/Ca\ 10^3 = 10.66 - 0.039\,T$)[7], or for aragonitic corals ($Sr/Ca\ 10^3 = 10.94 - 0.07\,T$)[5], but the value is similar to that of $16.37 - 0.22\,T$ obtained by analysis of whole otoliths from fish maintained in aquaria at a range of temperatures[6]. It appears, therefore, that biological factors are of much greater importance than simple inorganic fractionation in determining the concentrations of Sr in otolith carbonate, but that these factors are themselves temperature-dependent. However, variations in Sr concentration across the otolith section suggest that caution should be exercised in attempting to derive temperature data from analysis of whole otoliths.

This study demonstrated clearly that fluctuations in the concentrations of Sr, Na and K in fish otoliths, which were likely to be temperature-dependent and therefore related to season, corresponded with the visual banding which is accepted as being formed on an annual basis. It also showed that biological factors, presumably related to fish physiology, predominate over inorganic processes in determining trace element concentrations in otolith carbonate. Presumably the reasons for the changes in discrimination by the fish for and against the various ions will be clarified when more is known about seasonal variations in fish physiology, and their precise relationship to environmental conditions.

Inasmuch as otolith microchemistry provides an environmental record, long-lived species and fossil otoliths might provide evidence of past environments, despite the fact that the underlying biological processes are not yet defined. In addition, information on the life histories of individual fish, particularly those of migratory habit, should be contained within their otoliths, and it should be possible to reveal this information by microchemical analysis. The work described here has shown the value of FAB-SIMS as a tool for the elemental analysis of intact calcareous samples, giving high spatial resolution.

1 Carlstrom, D., Biol. Bull. *124* (1963) 441.
2 Degens, E. T., Deuser, W. G., and Haedrich, R. L., Mar. Biol. *2* (1969) 105.
3 Campana, S. E., and Neilson, J. D., Can. J. Fish. aquat. Sci. *42* (1985) 1014.
4 Summerfelt, R. C., and Hall, G. E., (Eds), Age and Growth of Fish. Iowa State University Press, Ames 1987.
5 Schneider, R. C., and Smith, S. V., Mar. Biol. *66* (1982) 121.
6 Radtke, R. L., Comp. Biochem. Physiol. *92A* (1989) 189.
7 Kinsman, D. J. J., and Holland, H. D., Geochim. cosmochim. Acta *33* (1969) 1.
8 Kalish, J. M., J. exp. mar. Biol. Ecol. *132* (1989) 151.
9 Devereux, I., Science *155* (1967) 1684.
10 Seyama, H., and Soma, M., Surf. Interface Anal. *15* (1990) 289.

0014-4754/91/11-12/1193-04$1.50 + 0.20/0

Inhibitory effects of flavonoids on several venom hyaluronidases

U. R. Kuppusamy and N. P. Das

Laboratory of Flavonoid Research, Department of Biochemistry, Faculty of Medicine, National University of Singapore, Kent Ridge Crescent, Singapore 0511

Received 30 November 1990; accepted 10 May 1991

Abstract. In vitro studies showed that the flavonoid aglycones apigenin, luteolin and kaempferol inhibited the hyaluronidase activity of five different venoms dose-dependently. They were also able to delay the venom action when injected into mice. Naringenin, catechin and flavonoid glycosides had no effect. The flavonoids with unsubstituted hydroxyl groups at C-positions 5, 7 and 4′, a double bond between carbons 2 and 3, as well as a ketone group at position 4, exhibited potent inhibitory actions on the venom hyaluronidases.

Key words. Flavonoids-hyaluronidase inhibition-venom action.

Flavonoids are benzo-γ-pyrone derivatives which are ubiquitous in plants[1] and they exhibit a great variety of pharmacological effects in biological systems[2,3]. They are also present as important constituents in several preparations used in folk medicine[4]. Various plant extracts have been reported to be able to neutralize the lethal activity of snake venoms[5,6]. Nevertheless, it must be borne in mind that such effects on the lethal activity do not necessarily correlate with the neutralization of specific pharmacological or enzymatic activities[7].

Hyaluronidase (EC 3.2.1.35), an enzyme widely distributed in mammalian testes, leech heads, invasive bacteria, and venoms of snakes, bees, scorpions and poisonous fishes[8,9] depolymerizes hyaluronic acid, a major constituent of animal connective tissues, which is essential for maintaining the integrity of the extracellular matrix[10]. Venoms of snake, bee and scorpion contain hyaluronidases with molecular weights ranging from 33,000 to 110,000[11,12], but little is known about the molecular structures of these enzymes. The activity of venom hyaluronidases shows a broad pH range in vitro, with an optimum pH at 4.0–5.0[9,10,12]. The end products of the action of these enzymes on hyaluronic acid are mainly tetrasaccharide units[9].

Tu and Hendon[11] supplied experimental evidence that this enzyme plays a role as a ‘spreading factor’ in the toxic action of venom. Despite the fact that hyaluronidase in itself is not a toxin[13], it may contribute to local or systemic envenomation by accelerating venom absorption and diffusion into the tissues of the victim[14]. Therefore, inhibition of this enzyme could play an important role in the therapy of venom poisoning.

Earlier work reported by Rodney et al.[15], and investigations carried out in our laboratory[16], showed that several structurally related flavonoids exhibited potent inhibition of bovine testis hyaluronidase. The present report is an investigation on the effects of a series of 13 flavonoids (table 1) on the hyaluronidase activity present in several commercially available snake, scorpion and bee venoms. In addition, venoms of two different species of snakes, namely the rattlesnake (*Crotalus atrox*) and the Malayan Cobra (*Naja naja sputatrix*), were used as models for an